

## First-principles study of the structural properties of Sn under pressure

B. H. Cheong and K. J. Chang

*Department of Physics, Korea Advanced Institute of Science and Technology, P.O. Box 150, Cheongryang, Seoul, Korea*

(Received 11 March 1991)

The structural properties of Sn at normal and high pressures are investigated using a self-consistent *ab initio* pseudopotential method. The structural stability of various phases including  $\alpha$ -Sn,  $\beta$ -Sn, simple hexagonal (sh), hexagonal close packed (hcp), body-centered tetragonal (bct), body-centered cubic (bcc), and face-centered cubic (fcc) is examined. The  $T=0$  scalar relativistic calculations show that  $\alpha$ -Sn undergoes a phase transition into  $\beta$ -Sn at 0.8 GPa. As pressure increases, we find successive phase transitions from  $\beta$ -Sn to bct at 19 GPa, to bcc at 46 GPa, and to hcp at 61 GPa. The transition sequence  $\beta$ -Sn  $\rightarrow$  bct  $\rightarrow$  bcc is consistent with experiment while bcc Sn was observed to be stable at room temperature up to 120 GPa. Examining two internal structural parameters, which induce a hcp-bcc transition, a small energy barrier that is less than thermal vibrational energy is found between bcc and hcp. This result suggests that the entropy term may be significant for the bcc phase at high pressures.

### I. INTRODUCTION

Among group-IV-A elements in the periodic table, C, Si, and Ge tend to form a diamond structure with strong covalent bonds. Since the valence  $s$  and  $p$  states in these elements are very close in energy, tetrahedrally coordinated bonding is preferred energetically via the change of hybridization from  $s^2p^2$  to  $sp^3$ . At normal pressure, although C was shown to be more stable in the graphite structure than in the diamond structure, the difference of energy ( $\cong 1-3$  mRy) between these two structures is extremely small.<sup>1</sup> Up to about 20 Mbar, no structural transition has been suggested for C.<sup>2</sup> For Si and Ge, many theoretical and experimental studies have shown that the semiconducting diamond phase transforms into the metallic  $\beta$ -Sn phase at similar pressures around 10 GPa.<sup>3-10</sup> Up to 1.25 Mbar, both Si and Ge undergo similar structural transformations from  $\beta$ -Sn to simple hexagonal (sh) to double-hexagonal close packed (dhcp).<sup>9</sup> However, the transition pressures between the metallic phases were found to be much higher in Ge than in Si. In Si a successive transition from dhcp to hexagonal close packed (hcp) and then to face-centered cubic (fcc) was found, while the hcp and fcc phases have not been identified for Ge.<sup>7-10</sup>

For heavier elements, however, the stable phases at atmospheric pressure are metallic; Sn and Pb are known to crystallize in the  $\beta$ -Sn and fcc phases, respectively, which appears as the high pressure phases in Si and Ge.<sup>11</sup> In Sn the diamond ( $\alpha$ -Sn) structure is more stable below 13°C and its band gap is actually zero.<sup>12</sup> Since cohesive energy decreases going down in the group-IV A column of the periodic table, the tetrahedral bonds of the diamond structure become relatively weakened in the heavier elements. Thus these bonds are effectively equivalent to those of the lighter elements at high pressures. Furthermore, since the energies of the valence  $s$  electrons in the heavier elements are much lower than those for the valence  $p$  states, the diamond phase with  $sp^3$  hybridization is less likely to occur and highly coordinated structures are favored.<sup>13</sup> In a previous pseudopotential calcu-

lation, the temperature-induced  $\alpha$ - to  $\beta$ -Sn transition in Sn was attributed to the significant entropy contribution to the free energy of the  $\beta$ -Sn phase.<sup>14</sup> As pressure increases, it has been observed that  $\beta$ -Sn transforms into a body-centered-tetragonal (bct) phase at 9.5 GPa.<sup>15</sup> At pressures between 40 and 50 GPa, a bct to body-centered-cubic (bcc) transition occurs and the bcc phase remains stable at room temperature up to 120 GPa.<sup>16</sup> However, there is little theoretical work on the high-pressure behavior of Sn.

In this paper we present the results of the *ab initio* pseudopotential calculations for the structural properties of Sn under pressure. The structural stability of the  $\alpha$ -Sn,  $\beta$ -Sn, sh, bct, bcc, hcp, and fcc phases is investigated for  $T=0$ . We also calculate the axial ratios for non cubic phases and find good agreement with available experimental data. The  $\alpha$ -Sn phase is found to be stable up to 0.8 GPa where a transition into  $\beta$ -Sn occurs. Although the energies of the  $\beta$ -Sn and sh phases are similar as previously found in Si and Ge,<sup>7,8</sup> no structural transition exists between the two phases. The  $\beta$ -Sn phase transforms into the bct phase at 19 GPa and then into the bcc phase at 46 GPa. This transition sequence is consistent with experimental observations. We find a further structural transition from bcc to hcp at 61 GPa, while the hcp phase has not been identified experimentally. Since the energies of the bcc and hcp phases are very close and a small energy barrier between bcc and hcp exists, its structural stability may be affected by temperature.

In Sec. II we briefly describe the method of calculation. In Sec. III the results of the calculations are presented and compared with other theoretical and experimental results. Conclusions are made in Sec. IV.

### II. METHOD

In the present calculations we use the first-principles total-energy pseudopotential method<sup>17</sup> within the local-density approximation.<sup>18</sup> The exchange and correlation potentials are approximated by the Wigner interpolation

formula.<sup>19</sup> This total-energy method using norm-conserving nonlocal pseudopotentials<sup>20</sup> has been successful in predicting the structural and dynamical properties of the group-IV elements C, Si and Ge.<sup>1-4,6-8,21</sup> To include relativistic corrections, we use the method proposed by Bachelet and Schlüter;<sup>22</sup> the angular-momentum- average pseudopotentials are employed in bulk calculations. Although spin-orbit interactions are significant in the electronic structure of Sn, we do not attempt to include these interactions because the calculations are extensive and the structural properties were shown to be insensitive to spin-orbit effects in other calculations.<sup>23</sup>

The total energy is calculated self-consistently in momentum space.<sup>24</sup> The (pseudo)wave functions are expanded in a plane-wave basis set with a kinetic energy cutoff ( $E_{PW}$ ) of up to 12.0 Ry. Increasing  $E_{PW}$  up to 25 Ry does not change the structural stability and relative energies are estimated to be accurate to within 0.1 mRy/atom. The summation of the charge density over the Brillouin zone is done using a uniform grid of  $k$  points. Since the crystal structures considered here are all metallic, a large number of  $k$  points are necessary to represent well the Fermi surfaces. Samplings of 10, 159, 150, 288, 120, 126, and 146  $k$  points in the irreducible Brillouin zone are chose for  $\alpha$ -Sn,  $\beta$ -Sn, sh, bct, bcc, hcp, and fcc, respectively. Compared with the bcc phase, the bct phase needs more  $k$  points because this lattice is less symmetric. Testing different samplings of  $k$  points, the maximum error in the total energy is estimated to be within 0.5 mRy/atom. For the noncubic  $\beta$ -Sn, sh, bct, and hcp structures, the total energies are optimized by varying the  $c/a$  ratio for a given volume. The axial ratio is found to vary as volume changes.

The ground-state properties, such as latticed constants, bulk moduli, and pressure derivatives of the bulk moduli, are obtained by fitting the computed total energies for various volumes to the Murnaghan's equation of state.<sup>25</sup> In this case the fitted energies are accurate to within 0.1 mRy/atom. By comparing the Gibbs free energies between two structures, we determine the structural stability and estimate the transition pressures and volumes for phase transformations.

We examine the transverse-acoustic (TA) phonon mode at the  $N$  point in the Brillouin zone of the bcc structure. This phonon mode is of particular interest because it is related to the bcc-hcp phase transformation, accompanied by uniform strain along the [001] direction.<sup>26</sup> Since the polarizations at the high-symmetry point are completely determined by symmetry, the frequency is evaluated with the use of the frozen-phonon approximation.<sup>21,27</sup> Within the harmonic approximation the phonon frequency is determined from the second-order coefficient at the phonon displacement.

### III. RESULTS

The equilibrium properties for  $\alpha$ -Sn and  $\beta$ -Sn are listed and compared with experiments in Table I. For both the phases, the calculated lattice constants ( $a_0$ ) and bulk moduli ( $B_0$ ) are in good agreement with the measured

TABLE I. Comparisons of the calculated lattice constants ( $a_0$ ), bulk moduli ( $B_0$ ), and their pressure derivatives ( $B'_0$ ) for various phases of Sn with other theoretical and experimental results.

	$a_0$ (Å)	$B_0$ (GPa)	$B'_0$	
$\alpha$ -Sn	6.40	51.2	4.0	Present calc.
	6.471	45.6		Other calc. <sup>a</sup>
	6.483 <sup>b</sup>	53 <sup>c</sup>		Expt.
$\beta$ -Sn	5.70	60.5	4.3	Present calc.
	5.733	62.9		Other calc. <sup>a</sup>
	5.812 <sup>d</sup>	57.9 <sup>e</sup>		Expt.
bct	4.79	57.8	4.1	Present calc.
bcc	4.62	57.5	4.2	Present calc.
		76.4	4.04	Expt. <sup>f</sup>
hcp	3.27	59.1	4.0	Present calc.
sh	3.13	60.1	4.1	Present calc.
fcc	4.64	57.4	4.0	Present calc.

<sup>a</sup>Reference 14.

<sup>d</sup>Reference 30.

<sup>b</sup>Reference 28.

<sup>e</sup>Reference 31.

<sup>c</sup>Reference 29.

<sup>f</sup>Reference 16.

values<sup>28-31</sup> to within less than 2% and 4%, respectively. For the pressure derivative of the bulk modulus ( $B'_0$ ), we find a value of 4.0 and 4.3 for  $\alpha$ -Sn and  $\beta$ -Sn, respectively, while experimental values are not available. Compared with a previous nonrelativistic calculation,<sup>14</sup> we obtain similar results for  $a_0$ , while improvements for  $B_0$  are noted. For other metallic bct, bcc, hcp, sh, and fcc phases, the calculated results for  $a_0$ ,  $B_0$ , and  $B'_0$  are also given in Table I. For bcc Sn the value of  $B_0$  is underestimated by about 30%, while a good agreement is found for  $B'_0$ , compared with the measured values.<sup>16</sup>

Figures 1(a) and 1(b) show the total energies semirelativistically calculated for  $T=0$  as a function of volume for various phases considered here. At zero pressure the  $\alpha$ -Sn phase is found to be the most stable and this structure changes into the  $\beta$ -Sn phase at a pressure of 0.8 GPa. The difference of the minimum energies for the  $\alpha$ - and  $\beta$ -Sn phases is about 2.5 mRy/atom, and this value is close to the previous nonrelativistic result of 2.9 mRy/atom.<sup>14</sup> It is known that the  $\alpha$ - to  $\beta$ -Sn transition takes place at atmospheric pressure just below room temperature (13°C).<sup>28</sup> Since the Debye temperature of  $\alpha$ -Sn is higher than that for  $\beta$ -Sn, the larger zero-point vibrational energy for  $\alpha$ -Sn reduces the transition pressure by 0.2 GPa. Furthermore, because the entropy term increases more rapidly for the  $\beta$ -Sn phase,<sup>14</sup> the pressure-induced  $\alpha$ - to  $\beta$ -Sn transition is expected to occur at lower pressures as temperature increases from zero.

The  $\beta$ -Sn phase is stable up to 19 GPa where a phase transition into a bct phase occurs with a volume change from  $0.82V_0$  to  $0.79V_0$  (see Table II), where  $V_0$  is the calculated equilibrium volume of the  $\beta$ -Sn phase. Although this structural transition is consistent with experiment, the calculated transition pressure overestimates the experimental value given in Table II by about 10 GPa. Because of this higher transition pressure, the transition volume is shown to be smaller than the measured value of

$0.88V_0$ . In both Si and Ge, the  $\beta$ -Sn phase was found to transform into a simple hexagonal phase. As is shown in Figs. 1(a) and 1(b), the total-energy curves for the  $\beta$ -Sn and sh phases lie very close in energy for volumes down to  $0.65V_0$ . This proximity of the energy curves was suggested to result from the structural similarity between the  $\beta$ -Sn and sh phases, which can be transformed via displa-

cive atomic motions.<sup>7</sup> However, the sh phase does not appear as a high-pressure phase in Sn.

Although the bct phase is more stable relative to the bcc and hcp structures below 19 GPa, their total energies shown in Fig. 1(a) are very close to within 0.7 mRy/atom for all volumes considered. It was shown that the atomic displacements specified in terms of optical phonon modes in  $\beta$ -Sn induces a change of phase from  $\beta$ -Sn to simple body-centered tetragonal.<sup>32</sup> In this case the axial ratio of the bct lattice is 0.77. As pressure is applied, since the crystal tends to form a close-packed structure, the  $\beta$ -Sn phase with coordination number (CN) 6 is likely to transform into the bct phase with CN=8. Then the bct phase has to have an increased axial ratio. Above 19 GPa, where the bct phase is more stable with respect to the  $\beta$ -Sn phase, the axial ratio of the bct phase is indeed found to be 0.9. As a consequence, the bct phase is expected to be stabilized prior to the formation of the bcc structure with the same CN and the larger axial ratio of  $c/a = 1$ .

At a higher pressure of 46 GPa, a phase transition from bct to bcc is found, which is consistent with the experimental observations.<sup>15,16</sup> Experiments showed a phase mixture of bct and bcc at pressures between 40 and 50 GPa, and above 50 GPa pure bcc Sn was observed.<sup>15</sup> For this transition the transition volume is estimated to be  $0.69V_0$  and this value is in good agreement with the measured value of  $0.70V_0$ .<sup>15</sup> In Fig. 2 the energy variation of the bct phase is plotted as a function of  $c/a$  and shows two local minima at  $c/a = 0.9$  and  $1.0$ , which correspond to the bct and bcc phases, respectively. At  $V = 0.76V_0$  the bct phase is more stable by about 0.35 mRy/atom than the bcc phase and the energy barrier for the bct-bcc transition is estimated to be about 0.5 mRy/atom. As volume decreases, the energy difference between bct and bcc decreases and becomes 0.1 mRy at  $V = 0.7V_0$ . At a more compressed volume of  $0.69V_0$ , the bcc phase is more stable over the bct phase; however, a small energy barrier still exists between the two structures.

Our calculations show a phase transition from bcc to hcp at 61 GPa. In this case the transition volume is cal-

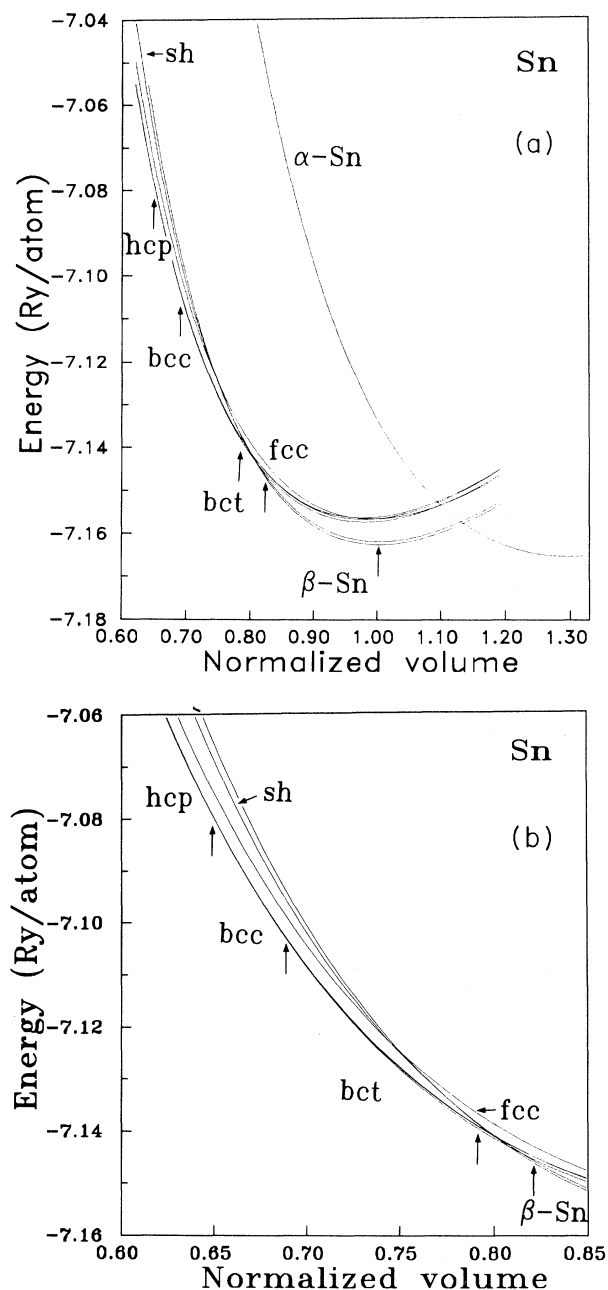


FIG. 1. (a) Crystal energies vs volume normalized by the calculated equilibrium volume of  $25.295 \text{ \AA}^3/\text{atom}$  for  $\beta$ -Sn. (b) Detailed structure of the curves in (a) near the phase transitions. The arrows indicate the transition volumes for the  $\beta$ -Sn to bct, the bct to bcc, and the bcc and hcp transitions.

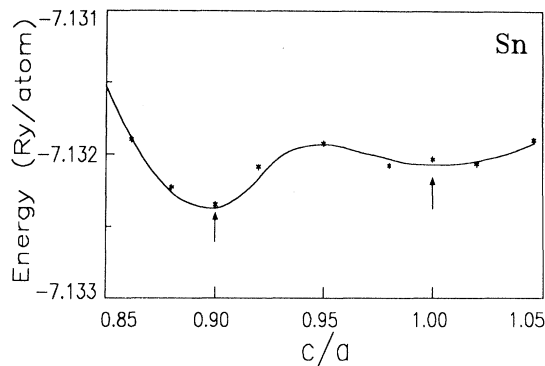


FIG. 2. Energies vs the axial ratio for the bct phase of Sn. A volume of  $19.26 \text{ \AA}^3/\text{atom}$  is chosen.

TABLE II. Transition pressures ( $P_t$ ) and transition volumes ( $V_t$ ) for  $T=0$ . Volumes are normalized by the equilibrium volume for the  $\beta$ -Sn phase ( $V_0=25.295 \text{ \AA}^3/\text{atom}$ ).

	$V_t$ ( $\alpha$ -Sn)		$V_t$ ( $\beta$ -Sn)		$V_t$ (bct)		$V_t$ (bcc)		$V_t$ (hcp)	$P_t$ (GPa)
Present calc.	1.28	→	0.99							0.8 (0.6) <sup>a</sup>
			0.82	→	0.79					19
					0.69	→	0.69			46
							0.65	→	0.65	61
Other calc. <sup>b</sup>			$\beta$ -Sn	→	bct					
			0.73							
					bct	→			hcp	
Expt. <sup>c</sup>			$\beta$ -Sn	→	bct					
			0.88		0.88					9.5
					bct	→	bcc			
					0.70		0.70			40–50

<sup>a</sup>Zero-point motions are included (see text).

<sup>b</sup>Reference 33.

<sup>c</sup>Reference 15.

culated to be  $0.65V_0$ . The stability of the hcp phase at high pressures was also suggested in other theoretical calculations.<sup>23</sup> However, there has been no experimental indication of the hcp phase at room temperature up to 120 GPa.<sup>16</sup> We find the hcp phase to be stable up to a maximum pressure of about 100 GPa considered here. Although a hcp phase was found to transform into a fcc phase in Si, the energies of the fcc phase in Sn lie higher than those for the hcp phase. Since our calculated energies for the bcc and hcp phases are too close, it is difficult to determine precisely the structural stability within our calculational accuracy. In addition, above 100 GPa, the  $d$  cores of Sn are likely to overlap. Thus, neglecting core-core interactions in the present calculations may affect the stability of the bcc and hcp phases.

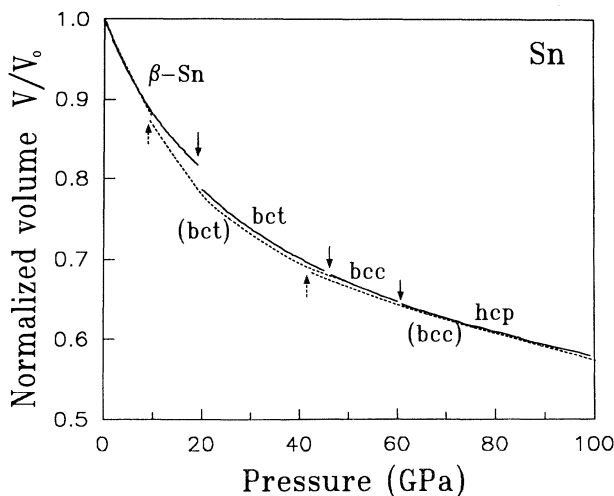


FIG. 3. Equation of state of Sn. Solid lines are our calculational results, while dotted lines denote the experimental results from Refs. 15 and 16. The arrows indicate the transition points.

In Fig. 3 the calculated equation of states is shown and compared with experiment. Except for pressures between 10 and 20 GPa, where a discrepancy between the calculated and measured transition pressures is found for the  $\beta$ -Sn to bct transition, generally good agreement is found between theory and experiment. The calculated  $c/a$  ratios for noncubic phases are given in Table III. For  $\beta$ -Sn, the calculated value of 0.545 is in good agreement with the measured value of 0.546.<sup>11</sup> For the bct phase, we find the  $c/a$  ratio to vary with volume; the ratio increases from 0.87 to 0.9 as volume changes from  $V_0$  to  $0.7V_0$ , compared with the experimental values ranging from 0.914 to 0.94.<sup>15,34</sup> For the hcp and sh phases, we find the  $c/a$  ratio to be 1.632 and 0.95, respectively. These values are very close to those previously found in Si and Ge.<sup>7,8</sup>

At atmospheric pressure, a temperature-induced hcp-bcc transition was found in Li, Na,<sup>35,36</sup> and Zr.<sup>37,38</sup> In these elements a hcp phase is more stable at low temperatures. As temperature increases, a phase changes into a bcc phase at 72, 36, and 1135 K for Li, Na, and Zr, respectively. In Sn, since the stable bcc phase up to 120 GPa was found at room temperature, it will be interesting to examine the stable phase at low temperatures. If the entropy term increases more significantly with tem-

TABLE III. Comparisons of the calculated  $c/a$  ratios for the  $\beta$ -Sn, bct, hcp, and sh phases of Sn with experimental values.

	$\beta$ -Sn	bct	hcp	sh
Calc.	0.545	0.87–0.90	1.632	0.95
Expt.	0.546 <sup>a</sup>	0.914 <sup>b</sup>		
		0.92–0.94 <sup>c</sup>		

<sup>a</sup>Reference 11.

<sup>b</sup>Reference 34.

<sup>c</sup>Reference 15.

perature for the bcc phase, the hcp phase can be a low-temperature phase as in Li, Na, and Zr.

By examining two internal structural parameters which induce a hcp-bcc phase transition, the energy barrier between bcc and hcp is calculated. Figure 4 shows displacive transformations from bcc to hcp. One of two structural degrees of freedom is characterized by displacing every second  $(110)_{\text{bcc}}$  planes by about  $(\sqrt{2}/6)a$ , where  $a$  is the bcc lattice constant, along the  $[1\bar{1}0]$  direction, corresponding to a transverse-acoustic- (TA-) phonon mode at the  $N$  point in the bcc Brillouin zone.<sup>26</sup> Then the  $(110)_{\text{bcc}}$  planes become the  $(001)$  planes of the hcp phase. The other parameter involves a contraction of the bcc lattice along the  $[001]$  axis until the bond angle ( $\theta$ ) on the basal planes changes from  $70.53^\circ$  to  $60^\circ$ . In Fig. 5 the variation of energy is plotted as a function of TA-phonon displacement  $\delta$  in units of  $(\sqrt{2}/24)a$  for various strains along the  $[001]$  direction. Without a strain ( $\theta=70.53^\circ$ ), the energy curve  $a$  corresponding to the  $N$ -point TA-phonon mode of the bcc phase, which is well fitted to a

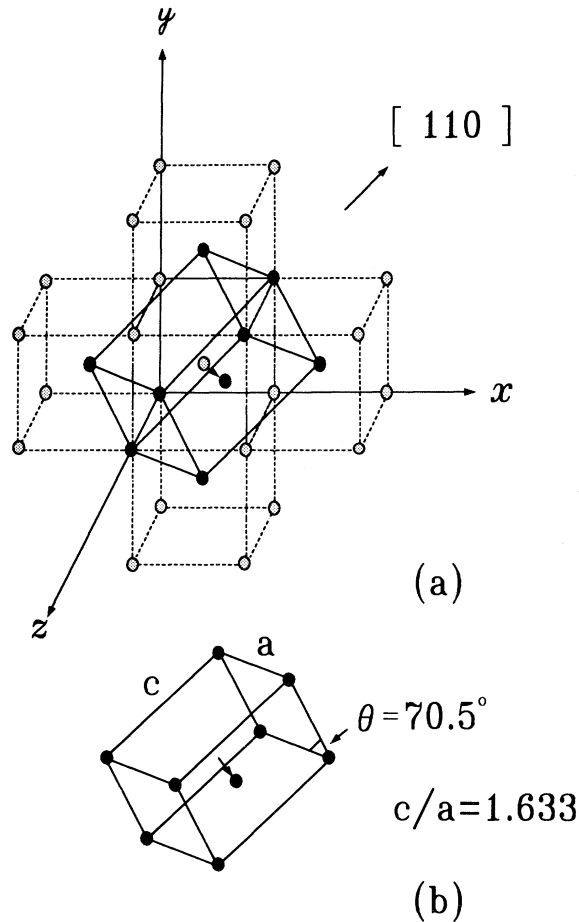


FIG. 4. A structural relationship between the bcc and hcp phases is shown in (a). The arrows indicate atomic displacements for the transverse-acoustic-phonon mode at the  $N$  point in bcc Sn. In (b) the bond angle is shown for the bcc plane. With the strain along the  $[001]$  direction, the bond angle is reduced to  $60^\circ$  to induce the hcp plane.

quadratic form, shows a minimum at zero phonon displacement. As strain increases, the bcc phase becomes unstable with respect to the displacive motion of the atomic positions. For a strain giving  $\theta=64^\circ$ , the minimum energy in curve  $b$  is found at an intermediate position between bcc and hcp. If  $\theta$  becomes  $60^\circ$ , which equals that of the hcp phase, the minimum energy in curve  $c$  is located at the phonon displacement of  $\delta=4.28$ , which induces exactly the hcp structure. In the curves  $a$  and  $c$ , the frequencies for the bcc and hcp phases are calculated to be 0.57 and 2.30 THz, respectively. As is shown in Fig. 5, for  $V=0.62V_0$  the energy difference between bcc and hcp is less than 1 mRy/atom. Along the lowest-energy curves, the energy barrier for the martensitic transformation from bcc to hcp is estimated to be about 1 mRy/atom, which is less than room-temperature energy. Although the entire phonon spectrum is required to see the entropy term, one-phonon-mode calculations indicate that the phonon mode of bcc Sn is softer than that for hcp. Then a larger entropy term at high temperatures may stabilize the bcc phase with respect to the hcp phase, as is found in experiments.

#### IV. CONCLUSIONS

We have shown that the  $T=0$  scalar relativistic pseudopotential calculations produce successfully the pressure-induced transition sequence  $\beta\text{-Sn}\rightarrow\text{bct}\rightarrow\text{bcc}$  in compressed Sn. The calculated ground-state properties of  $\alpha\text{-Sn}$  and  $\beta\text{-Sn}$  are in good agreement with experiment. For the  $\beta\text{-Sn}$  and bct phases, the axial ratios also agree

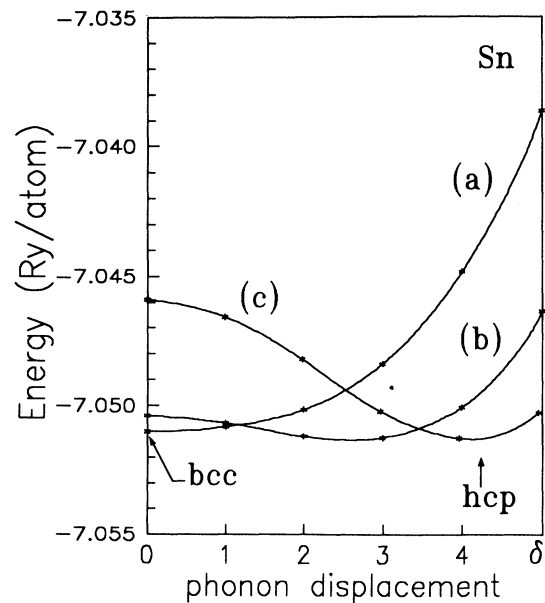


FIG. 5. Energy barriers from the bcc to the hcp phases for a volume of  $15.56 \text{ \AA}^3/\text{atom}$  where  $\delta$  is phonon displacement in units of  $(\sqrt{2}/24)a$ . As strain is applied along the  $[001]$  axis, the bond angle decreases from  $70.53^\circ$  (curve  $a$ ) to  $64^\circ$  (curve  $b$ ) and to  $60^\circ$  (curve  $c$ ).

well with experiment. Although experimentally bcc Sn was shown to be stable at room temperature up to 120 GPa, our calculations for  $T=0$  have predicted a bcc-hcp transition at a lower pressure. Because the energy difference between bcc and hcp is found to be less than thermal vibrational energy, it is suggested that the entropy term may be significant in the bcc phase stability at high pressures where the hcp phase is more stable at  $T=0$ . To clarify the discrepancy between theory and ex-

periment, further experimental work at low temperatures as well as extensive phonon-mode calculations are required.

#### ACKNOWLEDGMENT

This work was supported by the Korea Science and Engineering Foundation.

- 
- <sup>1</sup>M. T. Yin and M. L. Cohen, *Phys. Rev. B* **29**, 6996 (1984).  
<sup>2</sup>M. T. Yin and M. L. Cohen, *Phys. Rev. Lett.* **50**, 2006 (1983).  
<sup>3</sup>M. T. Yin and M. L. Cohen, *Solid State Commun.* **38**, 625 (1981).  
<sup>4</sup>M. T. Yin and M. L. Cohen, *Phys. Rev. Lett.* **45**, 1004 (1980).  
<sup>5</sup>H. Olijnyk, S. K. Sikka, and W. B. Holzapfel, *Phys. Lett.* **103A**, 137 (1984).  
<sup>6</sup>M. T. Yin and M. L. Cohen, *Phys. Rev. B* **26**, 5668 (1982).  
<sup>7</sup>K. J. Chang and M. L. Cohen, *Phys. Rev. B* **30**, 5376 (1984); **31**, 7819 (1985).  
<sup>8</sup>K. J. Chang and M. L. Cohen, *Phys. Rev. B* **34**, 8581 (1986).  
<sup>9</sup>Y. K. Vohra, K. E. Brister, S. Desgreniers, A. L. Ruoff, K. J. Chang, and M. L. Cohen, *Phys. Rev. Lett.* **56**, 1944 (1986).  
<sup>10</sup>S. J. Duclos, Y. K. Vohra, and A. L. Ruoff, *Phys. Rev. Lett.* **58**, 775 (1987).  
<sup>11</sup>R. W. G. Wyckoff, *Crystal Structures*, 2nd ed. (Interscience, New York, 1963), Vol. 1.  
<sup>12</sup>W. Paul, *J. Appl. Phys.* **32**, 2082 (1961).  
<sup>13</sup>N. E. Christensen, S. Satpathy, and Z. Pawlowska, *Phys. Rev. B* **34**, 5977 (1986).  
<sup>14</sup>J. Ihm and M. L. Cohen, *Phys. Rev. B* **23**, 1576 (1981).  
<sup>15</sup>H. Olijnyk and W. B. Holzapfel, *J. Phys. (Paris) Colloq.* **45**, Suppl. 11, C8-153 (1984).  
<sup>16</sup>S. Desgreniers, Y. K. Vohra, and A. L. Ruoff, *Phys. Rev. B* **39**, 10 359 (1989).  
<sup>17</sup>M. L. Cohen, *Phys. Scr.* **T1**, 5 (1982).  
<sup>18</sup>*Theory of the Inhomogeneous Electron Gas*, edited by S. Lundqvist and N. H. March (Plenum, New York, 1983), and references therein.  
<sup>19</sup>E. Wigner, *Trans. Faraday Soc.* **34**, 678 (1938).  
<sup>20</sup>D. R. Hamann, M. Schlüter, and C. Chiang, *Phys. Rev. Lett.* **43**, 1494 (1979).  
<sup>21</sup>M. T. Yin and M. L. Cohen, *Phys. Rev. B* **26**, 3259 (1982).  
<sup>22</sup>C. G. Bachelet and M. Schlüter, *Phys. Rev. B* **25**, 2103 (1982).  
<sup>23</sup>K. M. Rabe and J. D. Joannopoulos, *Phys. Rev. B* **32**, 2302 (1985).  
<sup>24</sup>J. Ihm, A. Zunger, and M. L. Cohen, *J. Phys. C* **12**, 4409 (1979).  
<sup>25</sup>F. D. Murnaghan, *Proc. Natl. Acad. Sci. U.S.A.* **30**, 244 (1944).  
<sup>26</sup>R. M. Wentzcovitch and M. L. Cohen, *Phys. Rev. B* **37**, 5571 (1988).  
<sup>27</sup>P. K. Lam and M. L. Cohen, *Phys. Rev. B* **25**, 6139 (1982).  
<sup>28</sup>D. L. Price and J. M. Rowe, *Solid State Commun.* **7**, 1433 (1969).  
<sup>29</sup>C. J. Buchenauer, M. Cardona, and F. H. Pollak, *Phys. Rev. B* **3**, 1243 (1971).  
<sup>30</sup>J. A. Rayne and B. S. Chandrasekhar, *Phys. Rev.* **120**, 1658 (1960).  
<sup>31</sup>S. N. Vaidya and G. C. Kennedy, *J. Phys. Chem. Solids* **31**, 2329 (1970).  
<sup>32</sup>M. J. P. Musgrave, *J. Phys. Chem. Solids* **24**, 557 (1963).  
<sup>33</sup>J. Hafner, *Phys. Rev. B* **10**, 4151 (1974).  
<sup>34</sup>J. D. Barnett, R. B. Bennion, and H. T. Hall, *Science* **141**, 1041 (1963).  
<sup>35</sup>T. Schneider and E. Stoll, *Solid State Commun.* **8**, 1729 (1970).  
<sup>36</sup>C. S. Rarrett, *Acta Crystallogr.* **9**, 671 (1956).  
<sup>37</sup>A. R. Kaufmann and T. T. Magel, in *Metallurgy of Zirconium*, edited by B. Lustman and F. Kerze (McGraw-Hill, New York, 1955).  
<sup>38</sup>E. Willaime and C. Massobrio, *Phys. Rev. Lett.* **63**, 2244 (1989).